PERIDOTITIC MANTLE XENOLITHS FROM KIMBERLITES ON THE EKATI DIAMOND MINE PROPERTY, NWT, CANADA

Andrew Menzies[1], Kalle Westerlund[2], John Gurney[1], Jon Carlson[3], Agnes Fung[4] and Tom Nowicki[5]

[1] Mineral Services, South Africa; [2] University of Cape Town, South Africa, [3] BHP Billiton Diamonds, Canada; [4] CF Minerals, Canada; [5] Mineral Services, Canada.

INTRODUCTION

The composition, structure and thermal state of the lithosphere beneath the Slave craton has been studied by analysing over 300 peridotitic mantle xenoliths entrained within kimberlites in the Lac de Gras area. The xenoliths were obtained from the Panda, Arnie, Mark, Pigeon, Sable, Leslie and Grizzly kimberlites located on the property of the Ekati Diamond Mine™, Northwest Territories, Canada. These kimberlites occur within 50 km of each other at surface, range between 47.5 and 53 Ma in emplacement age (for those dated), and are all diamondiferous to various degrees. The Panda kimberlite has been mined since the Ekati Diamond Mine™ opened in 1998.

SAMPLE DESCRIPTION

The samples were obtained from coarse concentrate and range in size up to 2 cm. Mineral compositions were determined by well-calibrated electron microprobe and LA-ICP-MS techniques. Due to the small size of the xenoliths and the resultant unrepresentative modal abundances of the various mineral phases, the mineral chemistry data were used as an aid in paragenesis classifications. For analytical purposes, the xenoliths were mounted as either grain (small chips of the various mineral phases) or xenolith probe mounts (see Table 1).

Scanning Electron Microscope (SEM) scans were undertaken for Mg and Al in all xenolith probe mounts. These scans allow the various mineral phases of olivine, orthopyroxene, garnet, clinopyroxene and chromite to be identified and precise points (i.e. core and rim) to be selected for analysis. The SEM scans and core-rim analyses provide an indication of spatial variation in composition and enable checking for both inter- and intra- grain homogeneity which is required for the application of geothermobarometers. Application of thermobarometry assumes equilibrium between the mineral phases present. This is unlikely to be the case for all the xenoliths and can only be partially verified by checking the compositional heterogeneity in mineral pairs (in cases where more than one mineral grain was mounted for a particular phase).

In this study, garnets from 43 xenolith mounts from Panda were analysed in situ for trace elements by LA-ICP-MS housed at the University of Cape Town. Four analyses were performed on each garnet – two in the core and two near the rim. The core - rim analyses will provide an indication of spatial variation in composition and enable a basic indication of intra-grain homogeneity on the trace level. A suite of twenty-two trace elements were determined: Sc, Ti, Mn, Ni, Ga, Rb, Sr, Y, Zr, La, Ce, Pr, Nd, Sm, Eu, Gd, Dy, Er, Yb, Lu, Hf and Pb.

The 43 xenoliths selected were chosen because of their large sample size and range in garnet Cr_2O_3-CaO compositions (Figure 1). Many of the specimens contain garnets that are Cr-rich (> 8 wt% Cr_2O_3) and highly sub-calcic. Whilst the garnet Cr_2O_3-CaO compositions of these 43 xenoliths vary, they do not represent the entire Cr_2O_3-CaO compositional range observed at the Panda kimberlite.

Table 1. Number of xenoliths from Ekati kimberlites analysed in this study.

Location	Analysed as grain mounts	Analysed as xenolith mounts
Pigeon	27	
Mark	21	
Arnie	44	
Panda	52	68
Sable	34	
Leslie	46	28
Grizzly	11	

MINERAL COMPOSITIONS

Major Elements

The garnets in xenoliths from the Panda, Arnie, Mark, Pigeon, Sable, Leslie and Grizzly kimberlites display a wide range of Cr_2O_3 and CaO contents (Figure 1),

including numerous high-Cr sub-calcic G10 synonymous with typical peridotitic diamond inclusion compositions. Panda and Leslie xenoliths display the greatest range in Cr_2O_3 and CaO concentrations. The majority of the garnets have low TiO_2 concentrations (Figure 2). The vast majority of the clinopyroxenes analysed are Cr-diopsides (Figure 3). However several samples record Cr_2O_3 concentrations of less than 0.5 wt%, not commonly associated with clinopyroxenes derived from lherzolite. There is a general overlap in clinopyroxene compositions from the various pipes. The Mg-numbers of orthopyroxene and olivine range above 0.90 and 0.91, respectively (Figure 4 and 5).

Trace Elements

The trace element compositions of the G10 garnets are relatively depleted in magmaphile elements compared to those of G9 garnets. For example, the G10 garnets yield extremely low concentrations of Ti, Zr, Y, Ga and Sc (Figure 6). All the high-Cr G10 garnets yield LREE enriched sinusoidal REE patterns (Figure 7). The few G9 garnets analysed to date for REE's display variable REE patterns that are relatively flat and show either a slight enrichment or a slight depletion of LREE relative to HREE (Figure 8). The trace element results indicate that the vast majority of garnets display little or no internal variation and may be regarded as homogeneous.

GEOTHERMOBAROMETRY (GTB)

Various geothermobarometer's applied to the multiphase xenoliths yield a vast range of temperatures (T) and pressures (P) indicating that these seven kimberlites sampled and entrained a large section of the lithosphere beneath Ekati™. Depending on the GTB used, pressures and temperatures may range from 650 to 1200 °C and 28 to 62 kbar. At any one individual kimberlite, the P-T range is generally narrower. For example, Panda and Pigeon yield predominantly high P-T xenoliths, whilst Grizzly yields predominantly low P-T xenoliths (Figure 9).

The P-T data show some scatter, but they indicate a coherent trend with no significant difference between different localities. Whilst the results of different GTB combinations yield varying pressure and temperature estimates for individual xenoliths as well as slightly different P-T trends, they all define an array that intersects the diamond stability field at approximately 900 °C and 42 kbar, equivalent to a model conductive geotherm of 37 mW/m^2 (Pollack and Chapman, 1977). In addition, there are no significant differences in the arrays displayed by xenoliths from individual kimberlites.

The largest xenolith data set from a single location is for the Panda kimberlite. At an assumed pressure of 40 kbar, the O'Neill and Wood thermometer (TONW79) yields a temperature range for harzburgites of 750 to 1000 °C (with one exception) and for lherzolites of 650 to 1150 °C (Figure 10). Even though the two peridotitic affinities overlap they display distinctly different modes. The lherzolites show a potential bi-modal distribution, with the dominant mode between 1000 to 1050 °C and the minor mode between 850 to 900 °C. In contrast, the harzburgites have a single mode of 900 to 950 °C, which is at the DSF-GSF boundary on a 37 mW/m^2 geotherm.

The Ni-in-garnet geothermometer of Ryan et al. (1996) yields similar results. The lherzolitic garnets yield T_{Ni}(Ryan96) temperatures ranging from 700 to 1150 °C, with no distinctive mode, most likely a function of the small data-set analysed to date; n = 12). The harzburgitic garnets cover a similar T_{Ni}(Ryan96) temperature range (700 to 1100 °C) with a distinctive mode between 950 and 1000 °C.

Various combinations of geothermobarometers are shown in Figure 9. Noticeably, in nearly all cases, the P-T points for all the localities lie between the model conductive geotherms for heatflows of 35 and 40 mW/m^2 (Pollack and Chapman, 1977), respectively. In addition, the P-T arrays do not follow these model conductive geotherms. They define a straight line that suggests a steeper temperature gradient than that of the model geotherm.

Pearson et al. (1998) studied mantle xenoliths from Lac de Gras area kimberlites (A154, DO-18 and DO-27) immediately to the south and south-east of the Ekati property. Whilst the Ekati results presented hear are broadly consistent with those of Pearson et al. (1998), there appear to be some key differences. In particular, on the basis of their GTB results, Pearson et al. (1998) proposed that this portion of the Slave craton lithosphere displays a change in the gradient of the paleogeotherm at ~ 900 – 1000 °C and that this coincides with the boundary between two compositionally distinct layers. Two possibilities were suggested to explain the apparent difference in geotherms for low-T xenoliths and high-T xenoliths (which is different from the "kink" geotherm observed at occurrences like Lesotho). It could either be a transient feature related to heating of the xenoliths at the time of kimberlite eruption or it may reflect two compositionally and thermally distinct layers in the upper mantle.

The results presented here do not provide clear evidence for such a stepped paleogeotherm in the lithosphere sampled by the Ekati kimberlites but yield a P-T array indicative of a continuous, relatively constant increase in temperature with depth. Whilst the Finnerty and Boyd (1986) / MacGregor (1974) GTB combination yields a P-T array that could be interpreted in terms of a stepped geotherm, this is equivocal and is not supported by the results of the other GTB methods applied. This suggests either that the paleogeothermal conditions beneath Ekati differed from those in the lithosphere sampled by the southern Lac de Gras kimberlites, or that the apparent stepped geotherm is a function of the particular GTB method and the geotherm model employed. Further investigation into the various GTB and model geotherm systematics is required to resolve this.

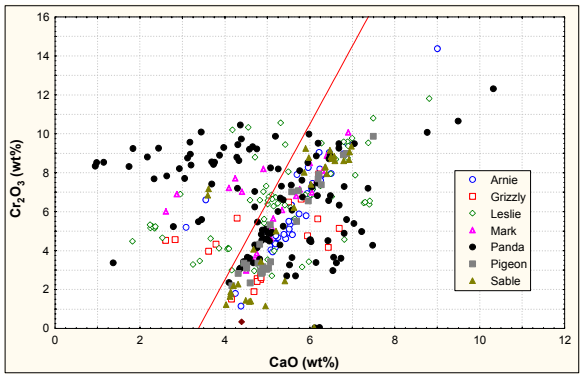

Figure 1: Garnet Cr_2O_3 and CaO compositions from xenoliths analysed in this study. The line of Gurney (1984) separates the grains into the G10 (sub-calcic) and G9 (calcic) fields.

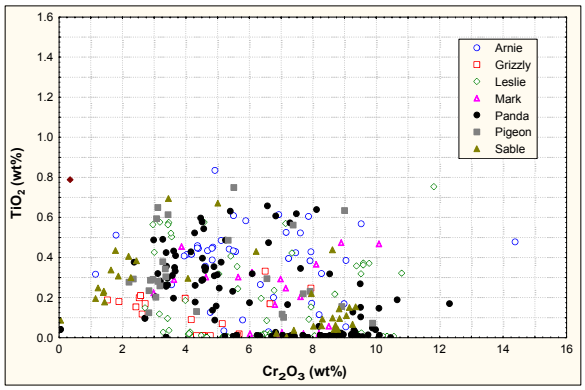

Figure 2: Garnet Cr_2O_3 and TiO_2 compositions from xenoliths analysed in this study.

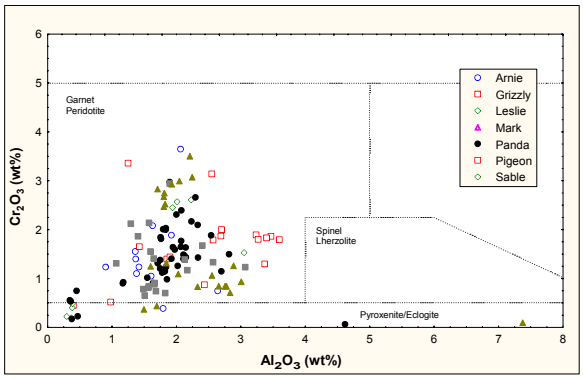

Figure 3: Clinopyroxene. Cr_2O_3 - Al_2O_3 compositions of clinopyroxenes from xenoliths analysed in this study. Fields are from Ramsay (1992).

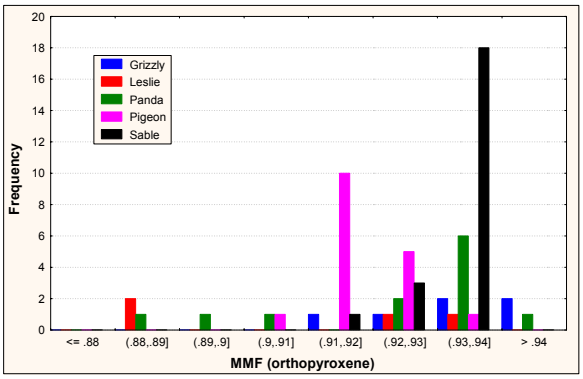

Figure 4: Mg number (Mg/Mg+Fe) of orthopyroxenes from xenoliths analysed in this study.

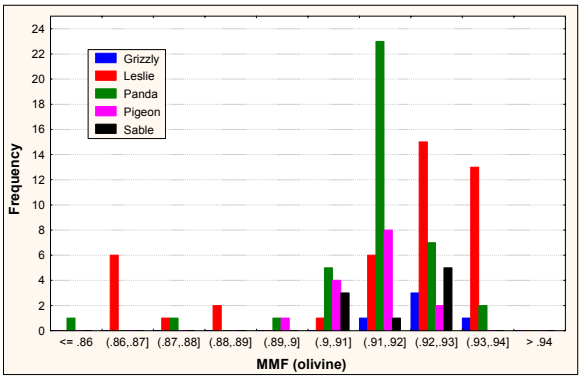

Figure 5: Mg number (Mg/Mg+Fe) of olivines from xenoliths analysed in this study.

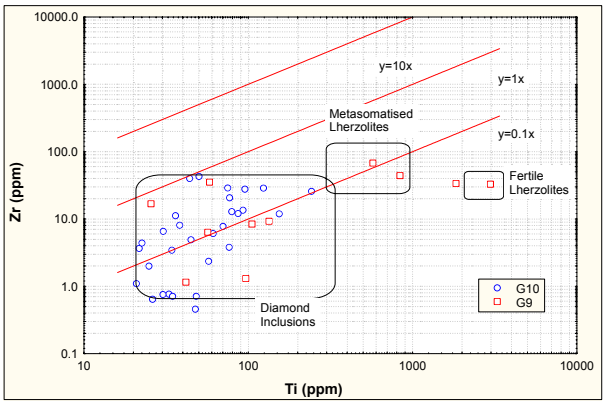

Figure 6. Panda garnet Ti-Zr compositions. The lines represent Ti/Zr isopleths. Fields are approximations from Shimuzu and Richardson (1987).

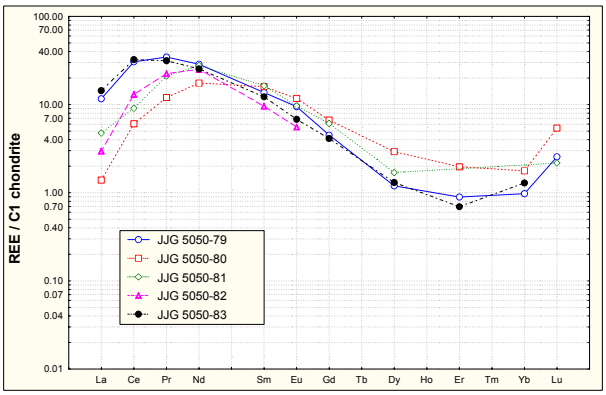

Figure 7: Typical REE pattern observed for the high-Cr G10 garnets analysed from Panda. Note the LREE enriched sinusodal pattern – a feature commonly observed in peridotitic diamond inclusions and diamond-bearing garnet peridotites.

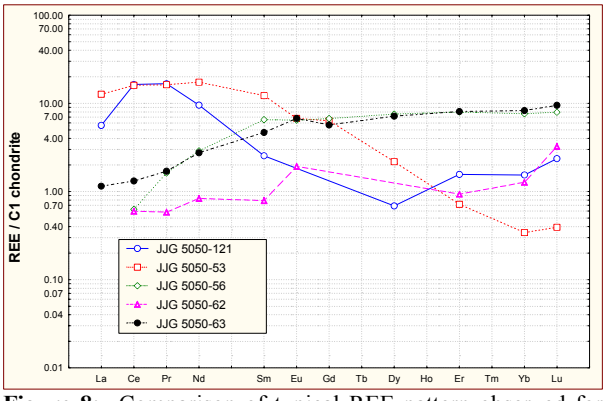

Figure 8: Comparison of typical REE pattern observed for the high-Cr G10 garnets analysed from Panda (5050-121 and JJG 5050-53) relative to the low-Cr G10 garnets (JJG 5050-62) and G9 garnets (JJG 5050-56 and JJG 5050-63) from Panda.

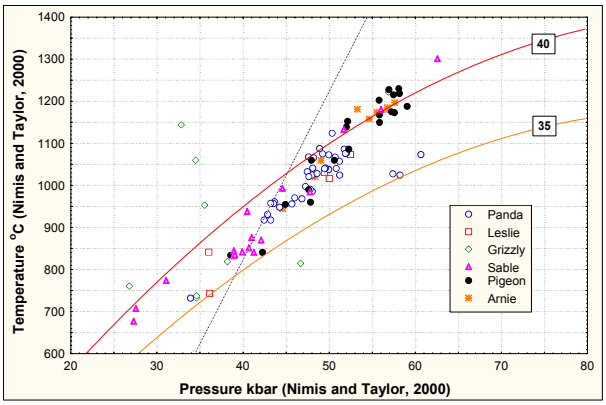

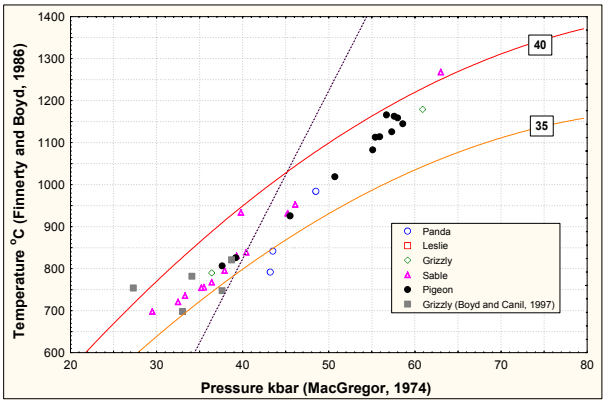

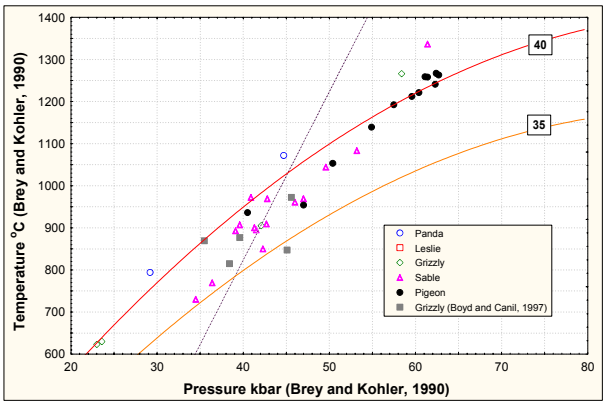

Figure 9: P-T results calculated using a variety of geothermobarometer combinations (as labeled on the respective axes) for peridotite xenoliths from Ekati kimberlites analysed in this study, in conjunction with the data for Grizzly from Boyd and Canil (1997). Model conductive geotherms labeled 35 and 40 mW/m^2 are after Pollack and Chapman (1977). The graphite/diamond equilibrium line is that of Kennedy and Kennedy (1976).

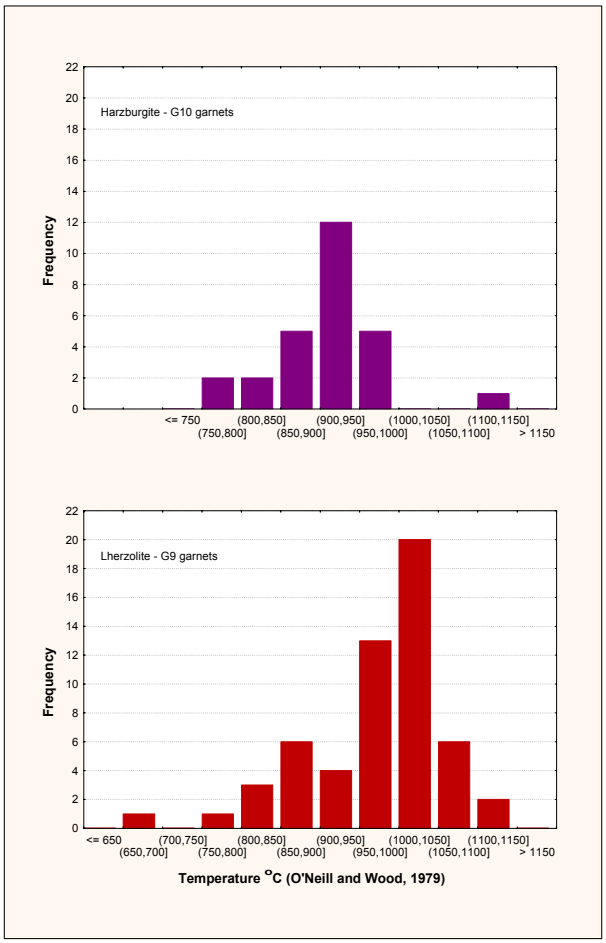

Figure 10: Histogram of calculated temperatures for harzburgitic and lherzolitic garnets from Ekati kimberlites using the O'Neill and Wood (1979) geothermometer at an assumed pressure of 40 kbar.

REFERENCES

Brey, G.P. and Köhler, T., 1990. Geothermobarometry in four-phase lherzolites: II New thermometers and practical assessment of existing thermobarometers. J. Petrol., 31, 1353-1378.

Boyd, F.R., and Canil, D., 1997. Peridotite xenoliths from the Slave Craton, Northwes Territories. Seventh Annual V.M. Goldschmit Conference abstracts, 34-35.

Finnerty, A.A., & Boyd, F.R., 1987. Thermobarometry for garnet peridotite xenoliths: a basis for mantle stratigraphy: In: Nixon, P.H. (ed.), Mantle Xenoliths, Wiley, New York, 381-412.

Gurney, J.J., 1984. A correlation between garnets and diamonds in kimberlites. In: Kimberlite Occurrence and Origin: A basis for conceptual models in exploration, Glover, J.E., & Harris, P.G., (eds.) Geology Department and University Extension, University of Western Australia, 8, 143-166.

Kennedy, C.S., and Kennedy, G.C., 1976. The equilibrium boundary between graphite and diamond. J. Geophys. Res. 81, 2467-2470.

MacGregor, I.D., 1974. The system MgO-Al2O3-SiO2: solubility of Al2O3 in enstatite for spinel and garnet peridotite compositions: Am. Min., 59, 110-119.

Nimis P. and Taylor W. R., 2000. Single clinopyroxene thermobarometry for garnet peridotites. Part 1. Calibration and testing of a Cr-in-Cpx barometer and an enstatite-in-Cpx thermometer. Contrib. Mineral. Petrol. 139, 541-554.

O'Neill, H.C, and Wood, B.J., 1979. An experimental study of Fe-Mg partitioning between garnet and olivine and its calibration as a geothermometer. Contrib. Mineral. Petrol., 70, 59-70.

Pearson, N.J., Griffin, B.J., Doyle, B.J., O'Reilly, S.Y., Van Acternergh, E, and Kivi, K, 1999. Xenoliths from kimberlite pipes of the Lac de Gras area, Slave craton, Canada. Proc. 7th Int Kimberlite Conf, Cape Town, Vol. 1, 644-658.

Pollack, H.N., and Chapman, D.S., 1977. On the regional variation of heat flow, geotherms, and lithospheric thickness. Tectonophysics 38, 279-296.

Ramsay, R.R., 1992, Geochemistry of Diamond Indicator Minerals. PHD Thesis, University of Western Australia, Perth.

Ryan, C.G., Griffin, W.L, and Pearson, N.J., 1996. Garnet geotherms: Pressure-temperature data from Cr-pyrope garnet xenocrysts in volcanic rocks. J. Geophys. Res., B3, 5611-5625.

Shimizu, N., and Richardson, S.H., 1987. Trace element abundance patterns of garnet inclusions in peridotitic suite diamonds. Geochim Cosmochim. Acta, 51, 755-758.

Contact: AH Menzies, PO Box 38668, Pinelands, 7430, South Africa, E-mail: Andrew.Menzies@minserv.co.za